Available online at www.sciencedirect.com

SciVerse ScienceDirect

Procedia Computer Science 00 (2020) 000–000

Procedia Computer Science

www.elsevier.com/locate/procedia

14th International Symposium "Intelligent Systems", INTELS'20, 14-16 December 2020, Moscow, Russia

Scissored pair control moment gyroscope inverted pendulum

Stanislav Aranovskiy[a], Igor Ryadchikov[b], Nikita Mikhalkov[c], Dmitry Kazakov[c], Alexey Simulin[c], Dmitry Sokolov[d,*]

[a] *Equipe Automatique, CentaleSupélec — IETR, Cesson-Sévigné, France*
[b] *Kuban State University, Krasnodar, Russia*
[c] *Neurolab LTD, Moscow, Russia*
[d] *Université de Lorraine, CNRS, Inria, LORIA, F-54000 Nancy, France*

Abstract

Motivated by non-anthropomorphic dynamic stabilization of a walking robot, we are working on a 2D inverted pendulum stabilized with a scissored pair of control moment gyroscopes. This inverted pendulum is a fair approximation of a robot, allowing us to study the dynamics in simplified settings. In this paper we propose a model for the pendulum; the model neglects all unessential terms and thus is suitable for analysis. We also propose a simple control law based on the linearization of the model and we validate it experimentally.

Peer-review under responsibility of the scientific committee of the 14th International Symposium "Intelligent Systems".

Keywords: Scissored-pair control moment gyroscope; inverted pendulum; bipedal gait

1. Introduction

The research problem of this paper is motivated by the walking robot we are currently developing in the Laboratory of Robotics and Mechatronics of the Kuban State University (refer to Fig. 1, left). This non-anthropomorphic robot has an auxiliary dynamic stabilization system which consists of two scissored pairs of control moment gyroscopes (CMG). The scissored pairs are orthogonal and thus the problem of vertical stabilization of the robot can be considered for each axis separately. Therefore, stabilization of the robot for one axis can be approximated with a simplified one-dimensional prototype. In this paper we consider such a prototype, which is a control moment gyroscope inverted pendulum (Fig. 2). Note that the robot has a modular design: the biped is equipped with four identical CMG cubes.

Control moment gyroscope is a widely used technological device that uses the reaction of a spinning wheel to external torques. Due to the advantages of a large ratio of produced torque to control torque and relatively low power consumption, CMGs have a wide range of applications, including vessel stabilisation [1], motorcycle and robot balancing [2], balancing aid for humans and bipedal exoskeletons [3,4], attitude steering system for the satellites [5] and underwater vehicles [6].

* Corresponding author. Tel.+33 3.83.59.20.77
E-mail address: dmitry.sokolov@univ-lorraine.fr

Peer-review under responsibility of the scientific committee of the 14th International Symposium "Intelligent Systems".

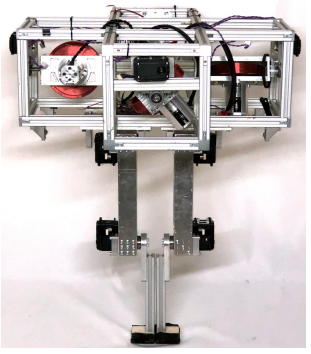

Fig. 1. We are developing a biped that uses four control moment gyroscopes (highlited in red) as an auxiliary stabilization system.

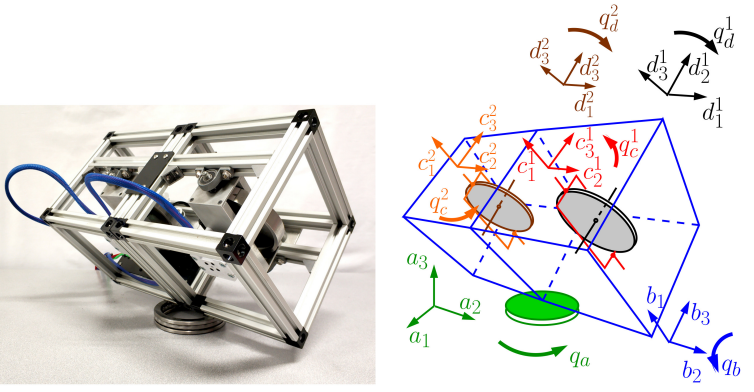

Fig. 2. **Left:** inverted pendulum hardware that we study in this paper. The pendulum consists of six bodies: body A (the thrust bearing), body B (the frame), bodies C^1 and C^2 (the single-axis gimbals), and, finally, bodies D^1 and D^2 (the flywheels). **Right:** corresponding notations. This configuration corresponds to $q_b = -\pi/4$ and $q_c^1 = q_c^2 = \pi/2$.

So, we are working on a 2D inverted pendulum stabilized with a scissored pair of control moment gyroscopes. This work extends the results[7,8] that were presented for a single CMG inverted pendulum. The main contribution of this paper is the model of the scissored pair system. Full Euler-Lagrange equations of the system are extremely cumbersome (few pages of fine print) even under numerous assumptions like symmetry of the bodies. We propose a much simpler model that neglects all unessential terms and thus is suitable for analysis. We validate the model by building a simple control law implemented in hardware.

The rest of the paper is organized as follows. In section 2 we present a model of the considered system. Next, in section 3 we present the state-feedback controller capable to stabilize the system if all states along with experimental validations of the results. Finally, possible further research directions are discussed in the concluding section 4.

2. Model Description

2.1. Mechanical system description

The considered inverted pendulum is shown in Fig. 2. In this paper we follow the notations from the manual of the model 750 control moment gyroscope commercialized by Educational Control Products company[9]. The pendulum consists of six bodies: body A (the thrust bearing, shown in green), body B (the frame, shown in blue), bodies C^1 and C^2 (the single-axis gimbals, shown in red and orange), and, finally, bodies D^1 and D^2 (the flywheels, shown in brown and black). We associate a basis with each of the bodies: $\{\vec{a}_1, \vec{a}_2, \vec{a}_3\}$, $\{\vec{b}_1, \vec{b}_2, \vec{b}_3\}$, $\{\vec{c}_1^1, \vec{c}_2^1, \vec{c}_3\}$, $\{\vec{c}_1^2, \vec{c}_2^2, \vec{c}_3^2\}$, $\{\vec{d}_1^1, \vec{d}_2^1, \vec{d}_3^1\}$ and $\{\vec{d}_1^2, \vec{d}_2^2, \vec{d}_3^2\}$, respectively. We assume that all the bodies are symmetric; so the inertia matrices are diagonal. Let us denote by $\mathrm{diag}(I_c, J_c, K_c)$ the inertia matrix (w.r.t the center of mass) of the bodies C^1 and C^2; and by $\mathrm{diag}(I_d, J_d, K_d)$ the inertia matrix of the bodies D^1 and D^2. In the same manner, we denote the inertia matrix of the body A as $\mathrm{diag}(I_a, J_a, K_a)$. As for the body B, the frame consists of two identical cubes, and we denote by I_b, J_b and K_b the principal moments of inertia of each half of the frame w.r.t. the center of mass of each cube.

We denote by q_a the angle of rotation between the "north" direction and the body A; the angle of the body B with respect to the vertical is denoted as q_b; the angle of the bodies C^1 and C^2 with respect to the body B are denoted as q_c^1 and q_c^2; and the angle of the bodies D^1 and D^2 with respect to the body C^1 and C^2 are denoted as q_d^1 and q_d^2. The configuration shown in Fig. 2 corresponds to the angles $q_b = -\pi/4$ and $q_c^1 = q_c^2 = \pi/2$. Note that the equilibrium position of an actual device may be subject to external disturbances and sensor displacement; therefore, for our system we model the equilibrium point as $q_b = -\pi/4 - e$, where e is the unknown (small) bias. The notations and the corresponding hardware parameters are summarized in the Table 1.

Table 1. Hardware parameters

Description	Symbol	Value
Total mass, kg	m	2.62
Cube edge length, m	l	0.19
Moments of inertia, kg·m^2:		
of the body A	K_a	$6 \cdot 10^{-4}$
of the body B	$[I_b,\ J_b,\ K_b]$	$[13\ 10\ 13] \cdot 10^{-3}$
of the body C	$[I_c,\ J_c,\ K_c]$	$[2.6\ 10\ 10] \cdot 10^{-4}$
of the body D	$[I_d,\ J_d,\ K_d]$	$[5.6\ 11\ 5.6] \cdot 10^{-4}$
Disk D velocity, rad/s	ω_d	314
Equilibrium position bias, rad	e	unknown

With these definitions, the vectors of angular velocities can be found as:

$$\vec{\omega}_a = \begin{bmatrix} 0 \\ 0 \\ \dot{q}_a(t) \end{bmatrix}, \qquad \vec{\omega}_b = \begin{bmatrix} 0 \\ \dot{q}_b(t) \\ 0 \end{bmatrix} + R_{AB}(q_b) \times \vec{\omega}_a, \qquad \vec{\omega}_c^1 = \begin{bmatrix} \dot{q}_c^1(t) \\ 0 \\ 0 \end{bmatrix} + R_{BC}(q_c^1) \times \vec{\omega}_b,$$

$$\vec{\omega}_d^1 = \begin{bmatrix} 0 \\ \dot{q}_d^1(t) \\ 0 \end{bmatrix} + R_{CD}(q_d^1) \times \vec{\omega}_c^1, \qquad \vec{\omega}_c^2 = \begin{bmatrix} \dot{q}_c^2(t) \\ 0 \\ 0 \end{bmatrix} + R_{BC}(q_c^2) \times \vec{\omega}_b, \qquad \vec{\omega}_d^2 = \begin{bmatrix} 0 \\ \dot{q}_d^2(t) \\ 0 \end{bmatrix} + R_{CD}(q_d^2) \times \vec{\omega}_c^2.$$

where R_{AB}, R_{BC} and R_{CD} are the transformations between the bases of corresponding bodies:

$$R_{AB}(\alpha) = \begin{bmatrix} \cos\alpha & 0 & -\sin\alpha \\ 0 & 1 & 0 \\ \sin\alpha & 0 & \cos\alpha \end{bmatrix}, \qquad R_{BC}(\alpha) = \begin{bmatrix} 1 & 0 & 0 \\ 0 & \cos\alpha & \sin\alpha \\ 0 & -\sin\alpha & \cos\alpha \end{bmatrix}, \qquad R_{CD}(\alpha) = \begin{bmatrix} \cos\alpha & 0 & -\sin\alpha \\ 0 & 1 & 0 \\ \sin\alpha & 0 & \cos\alpha \end{bmatrix}.$$

When clear from the context, in the sequel the argument of time is omitted. Then the parallel axis theorem allows us to write the total kinetic energy of the system as:

$$T = \frac{1}{2}\Big(\vec{\omega}_d^{1\top} \times \mathrm{diag}(I_d, J_d, K_d) \times \vec{\omega}_d^1 + \vec{\omega}_c^{1\top} \times \mathrm{diag}(I_c, J_c, K_c) \times \vec{\omega}_c^1 + \vec{\omega}_d^{2\top} \times \mathrm{diag}(I_d, J_d, K_d) \times \vec{\omega}_d^2 +$$
$$\vec{\omega}_c^{2\top} \times \mathrm{diag}(I_c, J_c, K_c) \times \vec{\omega}_c^2 + 2\vec{\omega}_b^\top \times \mathrm{diag}\left(I_b, J_b + \frac{1}{2}ml^2, K_b\right) \times \vec{\omega}_b + \vec{\omega}_a^\top \times \mathrm{diag}\left(I_a, J_a, K_a + \frac{1}{2}ml^2\right) \times \vec{\omega}_a\Big).$$

The potential energy is given by $P = \sqrt{2}mlg\cos(q_b + \pi/4 + e)$. Therefore the Lagrangian can be written as $\mathcal{L} = T - P$. The torques τ_c^1, τ_c^2, τ_d^1 and τ_d^2 are applied to the bodies C^1, C^2, D^1 and D^2, respectively; thus the dynamics obeys the Euler–Lagrange equations:

$$\begin{cases} \frac{d}{dt}\left(\frac{\partial \mathcal{L}}{\partial \dot{q}_a}\right) - \frac{\partial \mathcal{L}}{\partial q_a} &= 0 \\ \frac{d}{dt}\left(\frac{\partial \mathcal{L}}{\partial \dot{q}_b}\right) - \frac{\partial \mathcal{L}}{\partial q_b} &= 0 \\ \frac{d}{dt}\left(\frac{\partial \mathcal{L}}{\partial \dot{q}_c^1}\right) - \frac{\partial \mathcal{L}}{\partial q_c^1} &= \tau_c^1 \\ \frac{d}{dt}\left(\frac{\partial \mathcal{L}}{\partial \dot{q}_c^2}\right) - \frac{\partial \mathcal{L}}{\partial q_c^2} &= \tau_c^2 \\ \frac{d}{dt}\left(\frac{\partial \mathcal{L}}{\partial \dot{q}_d^1}\right) - \frac{\partial \mathcal{L}}{\partial q_d^1} &= \tau_d^1 \\ \frac{d}{dt}\left(\frac{\partial \mathcal{L}}{\partial \dot{q}_d^2}\right) - \frac{\partial \mathcal{L}}{\partial q_d^2} &= \tau_d^2 \end{cases} \tag{1}$$

These equations can be also written in the matrix form

$$M^\dagger(q)\ddot{q} + C^\dagger(q, \dot{q}) + G^\dagger(q) = \tau - F_r^\dagger(\dot{q}),$$

where

$$q := \left[q_a\ q_b\ q_c^1\ q_c^2\ q_d^1\ q_d^2\right]^\top,$$
$$\tau := \left[0\ 0\ \tau_c^1\ \tau_c^2\ \tau_d^1\ \tau_d^2\right]^\top,$$

and $F_r^\dagger(\dot{q})$ corresponds to friction and other resistance forces.

Assumption 1 (Mechanical symmetry)**.** *We assume that the following mechanical symmetries hold*

$$K_b = J_b = I_b,\ K_c = J_c,\ K_d = I_d.$$

Under Assumption 1, the matrix $M^\dagger$ takes the form

$$M^\dagger(q) = \begin{bmatrix} m_{11} & m_{12} & m_{13} & m_{14} & m_{15} & m_{16} \\ m_{12} & m_{22} & 0 & 0 & J_d\cos(q_c^1) & J_d\cos(q_c^2) \\ m_{13} & 0 & I_c + I_d & 0 & 0 & 0 \\ m_{14} & 0 & 0 & I_c + I_d & 0 & 0 \\ m_{15} & J_d\cos(q_c^1) & 0 & 0 & J_d & 0 \\ m_{16} & J_d\cos(q_c^2) & 0 & 0 & 0 & J_d \end{bmatrix}, \tag{2}$$

where

$$\begin{aligned} m_{11} &= (I_d - J_d)\cos^2(q_b)\cos^2(q_{c1}) + (I_d - J_d)\cos^2(q_b)\cos^2(q_{c2}) \\ &\quad + (2J_c - 2I_d - 2I_c + 2J_d)\cos^2(q_b) + \frac{m l^2}{2} + 2I_b + 2I_c + 2I_d + K_a, \\ m_{12} &= -\cos(q_b)(I_d - J_d)\left(\frac{\sin(2q_{c1})}{2} + \frac{\sin(2q_{c2})}{2}\right), \\ m_{13} &= -\sin(q_b)(I_c + I_d), \\ m_{14} &= m_{13}, \\ m_{15} &= J_d\cos(q_b)\sin(q_{c1}), \\ m_{16} &= J_d\cos(q_b)\sin(q_{c2}), \\ m_{22} &= (J_d - I_d)\cos^2(q_{c1}) + (J_d - I_d)\cos^2(q_{c2}) + m l^2 + 2I_b + 2I_d + 2J_c. \end{aligned}$$

2.2. Local controllers of bodies C and D

We assume that the torque τ is generated by local servo drives that operate in fast time scale compared to the dynamics of the whole system. The effect of these controllers is described in the following assumptions.

Assumption 2 (Local control of bodies D^1 and D^2)**.** *For the bodies D^1 and D^2, the local controllers ensure constant velocities*

$$\dot{q}_d^1 = \omega_d,\ \dot{q}_d^2 = -\omega_d$$

for some constant ω_d; thus, $\ddot{q}_d^1 = \ddot{q}_d^2 = 0$ for all t.

Assumption 3 (Local control of bodies C^1 and C^2)**.** *For the bodies C^1 and C^2, the local controllers ensure the perfect reference tracking*

$$\dot{q}_c^1 = u_1,\ \dot{q}_c^2 = u_2,$$

where u_1 and u_2 are further considered as the new input signals.

Assumption 4 (Neglectable impact of m_{13}, m_{14})**.** *Formally, under Assumption 3 the accelerations of the bodies C^1 and C^2 given by $\ddot{q}_c^1 = \dot{u}_1$ and $\ddot{q}_c^2 = \dot{u}_2$ are affecting the dynamics of the body A due to the coefficients m_{13} and m_{14} of the matrix M* (2)*. However, for the considered system these coefficients are small compared to other entries of the matrix M. Thus, in what follows we neglect this effect and assume*

$$m_{13} = m_{14} = 0.$$

Note that we apply this assumption for control design and model simplification, but not necessarily for simulations.

Taking into account these assumptions, the model can be reduced to

$$\dot{q}_a = \omega_a, \quad \dot{q}_b = \omega_b, \quad \dot{q}_{c,1} = u_1, \quad \dot{q}_{c,2} = u_2,$$

$$M(q)\begin{bmatrix}\dot{\omega}_a\\ \dot{\omega}_b\end{bmatrix} = -C(q,\dot{q}),$$

where

$$M := \begin{bmatrix}m_{11}\ m_{12}\\ m_{12}\ m_{22}\end{bmatrix},\ C := \begin{bmatrix}I_2\ 0\end{bmatrix}\left(C^{\dagger}(q,\dot{q}) + G^{\dagger}(q) + F_r^{\dagger}(\dot{q})\right) = \begin{bmatrix}C_1\\ C_2\end{bmatrix},$$

and $\dot{q}_{c,1}$ and $\dot{q}_{c,1}$ denotes $\dot{q}_c^1$ and $\dot{q}_c^1$, respectively.

2.3. Model simplification

Define the new parameters

$$\begin{gathered} p_1 = 2I_b + 2I_c + 2I_d + K_a + \frac{m\,l^2}{2},\ p_2 = 2I_b + 2I_d + 2J_c + ml^2,\\ p_3 = J_c + J_d - I_c - I_d,\ p_4 = J_d - I_d\\ p_5 = I_c + J_d,\ p_6 = I_c + 2I_d - J_d. \end{gathered} \tag{3}$$

Rewrite now the matrix M as $M := M_0 + M_1(q)$, where

$$M_0 := \begin{bmatrix}p_1 & 0\\ 0 & p_2\end{bmatrix}, \quad M_1(q) := \begin{bmatrix}\left(2p_3 - p_4\left(\cos^2(q_{c,1}) + \cos^2(q_{c,2})\right)\right)\cos^2(q_b) & \frac{1}{2}p_4\cos(q_b)\left(\sin(2q_{c,1}) + \sin(2q_{c,2})\right)\\ \frac{1}{2}p_4\cos(q_b)\left(\sin(2q_{c,1}) + \sin(2q_{c,2})\right) & p_4\left(\cos^2(q_{c,1}) + \cos^2(q_{c,2})\right)\end{bmatrix}.$$

For our setup it can be shown that for all feasible q it holds

$$\|\left(M_0 + M_1(q)\right)^{-1} - M_0^{-1}\| \le 0.04\|M_0^{-1}\|$$

Thus, for simplicity in what follows we will apply the following simplification:

$$M^{-1}(q) \approx M_0^{-1}.$$

The vector C has the following expression:

$$\begin{aligned} C = \Big(& f_r(\omega_a) - 2\,p_3\,\omega_a\,\omega_b\,\sin(2\,q_b) - J_d\,\omega_b\,\omega_d\,\sin(q_b)\,(\sin(q_{c1}) - \sin(q_{c2}))\\ &+ p_4\,\omega_a\,\omega_b\,\sin(2\,q_b)\left(\cos^2(q_{c1}) + \cos^2(q_{c2})\right) - p_4\frac{1}{2}\omega_b{}^2\,\sin(q_b)\,(\sin(2\,q_{c1}) + \sin(2\,q_{c2}))\\ &+ p_4\,\omega_a\,\cos^2(q_b)\,(u_1\,\sin(2\,q_{c1}) + u_2\,\sin(2\,q_{c2})) + 2p_4\,\omega_b\,\cos(q_b)\left(u_1\,\cos^2(q_{c1}) + u_2\,\cos^2(q_{c2})\right)\\ &+ J_d\,\omega_d\,\cos(q_b)\,(u_1\,\cos(q_{c1}) - u_2\,\cos(q_{c2})) - p_5\omega_b\,\cos(q_b)\,(u_1 + u_2),\\ &- \sqrt{2}\,g\,l\,m\,\sin\left(q_b + \frac{\pi}{4} + e\right) + p_3\,\omega_a{}^2\,\sin(2\,q_b) + J_d\,\omega_a\,\omega_d\,\sin(q_b)\,(\sin(q_{c1}) - \sin(q_{c2}))\\ &- p_4\,\frac{1}{2}\omega_a{}^2\,\sin(2\,q_b)\left(\cos^2(q_{c1}) + \cos^2(q_{c2})\right) - p_4\,\omega_b\,(u_1\,\sin(2\,q_{c1}) + u_2\,\sin(2\,q_{c2}))\\ &- J_d\,\omega_d\,(u_1\,\sin(q_{c1}) - u_2\,\sin(q_{c2})) + 2\,p_4\,\omega_a\,\cos(q_b)\left(u_1\,\cos^2(q_{c1}) + u_2\,\cos^2(q_{c2})\right) - p_6\omega_a\,\cos(q_b)\,(u_1 + u_2)\Big)^{\top}. \end{aligned}$$

Let us define C_0 as follows:

$$\begin{aligned} C_0 := \Big(& f_r(\omega_a) - J_d\,\omega_b\,\omega_d\,\sin(q_b)\,(\sin(q_{c1}) - \sin(q_{c2})) + J_d\,\omega_d\,\cos(q_b)\,(u_1\,\cos(q_{c1}) - u_2\,\cos(q_{c2})),\\ &- \sqrt{2}\,g\,l\,m\,\sin\left(q_b + \frac{\pi}{4} + e\right) + J_d\,\omega_a\,\omega_d\,\sin(q_b)\,(\sin(q_{c1}) - \sin(q_{c2})) - J_d\,\omega_d\,(u_1\,\sin(q_{c1}) - u_2\,\sin(q_{c2}))\Big)^{\top}. \end{aligned}$$

In our setup the velocities are bounded: it is reasonable to assume that $|w_a|$ and $|w_b|$ are inferior to 10 rad/s. Under this assumption it is easy to see that $\|C - C_0\| < 10^{-3}$ and that we can apply the following simplification:

$$C \approx C_0.$$

Thus, the model can be reduced to

$$M_0 \begin{bmatrix} \dot{\omega}_a \\ \dot{\omega}_b \end{bmatrix} = -C_0(q, \dot{q}), \tag{4}$$

3. Linearization-based stabilization

For the system (4), the desired equilibrium is defined as

$$\Omega_0 := \left\{ \omega_a = 0,\ q_b = -\frac{\pi}{4} - e,\ \omega_b = 0,\ q_{c1} = q_{c2} = \frac{\pi}{2} \right\}.$$

In what follows we say that a control law (locally) stabilizes the system (4) if under this control law the point Ω_0 is (locally) attractive. Define

$$x_1 = q_a, \quad x_2 = \dot{q}_a, \quad x_3 = q_b + \frac{\pi}{4} + e, \quad x_4 = \dot{q}_b, \quad x_5 = q_{c1} - \frac{\pi}{2}, \quad x_6 = q_{c2} - \frac{\pi}{2}. \tag{5}$$

Then the system's dynamics can be rewritten as

$$\begin{bmatrix} \dot{x}_1 \\ \dot{x}_2 \\ \dot{x}_3 \\ \dot{x}_4 \\ \dot{x}_5 \\ \dot{x}_6 \end{bmatrix} = \begin{bmatrix} x_2 \\ f_a(x,u) \\ x_4 \\ f_b(x,u) \\ u_1 \\ u_2 \end{bmatrix}, \tag{6}$$

where $f_a(\vec{0}, \vec{0}) = f_b(\vec{0}, \vec{0}) = 0$ and the origin is an equilibrium (for zero input). The function f_a and f_b are defined as follows:

$$f_a(x,u) := \frac{-f_r(\omega_a) + J_d\, \omega_b\, \omega_d\, \sin\left(x_3 - \frac{\pi}{4} - e\right) (\cos x_5 - \cos x_6) - J_d\, \omega_d\, \cos\left(x_3 - \frac{\pi}{4} - e\right) (u_2 \sin x_6 - u_1 \sin x_5)}{p_1}$$

$$f_b(x,u) := \frac{\sqrt{2}\, g\, l\, m \sin x_3 - J_d\, \omega_a\, \omega_d \sin\left(x_3 - \frac{\pi}{4} - e\right) (\cos x_5 - \cos x_6) + J_d\, \omega_d\, (u_1 \cos x_5 - u_2 \cos x_6)}{p_2}$$

The control goal can be achieved if we start from the initial position $x_5(0) = x_6(0) = 0$ and impose a symmetry of control $u_1(t) = -u_2(t)$. Then obviously $x_6(t) = -x_5(t)$, $\omega_a(t) = 0$, and the system (6) can be reduced as follows:

$$\begin{bmatrix} \dot{x}_3 \\ \dot{x}_4 \\ \dot{x}_5 \end{bmatrix} = \begin{bmatrix} x_4 \\ \frac{\sqrt{2}\, g\, l\, m \sin x_3 + 2 J_d\, \omega_d\, u_1 \cos x_5}{p_2} \\ u \end{bmatrix} \tag{7}$$

The state variable x_5 can be computed through the measurements of the signal q_{c1}; however, since the offset e is not known, the signal x_3 can not be computed. Thus, we define the vector of measurements as

$$y = \begin{bmatrix} q_b + \frac{\pi}{4} \\ q_{c1} - \frac{\pi}{2} \end{bmatrix} = \begin{bmatrix} x_3 - e \\ x_5 \end{bmatrix}. \tag{8}$$

Then the control goal is to find a control law that stabilizes (7) at the origin using the measurements y. A common practice to stabilize a (sufficiently well-behaved) nonlinear system is to linearize the system around the desired

equilibrium. For the system (7) such equilibrium is given by $x = 0$, $u = 0$. Let us define

$$A := \begin{bmatrix} 0 & 1 & 0 \\ \frac{\sqrt{2}glm}{p_2} & 0 & 0 \\ 0 & 0 & 0 \end{bmatrix}, \quad B := \begin{bmatrix} 0 \\ \frac{2J_d\omega_d}{p_2} \\ 1 \end{bmatrix} \tag{9}$$

Then the linearization of (7) around the origin is given by $\dot{x} = Ax + Bu_1$. It is tempting to use the state-feedback static control

$$u_1 := -K \begin{bmatrix} y_1 & x_2 & y_2 \end{bmatrix} = -Kx - k_1 e, \tag{10}$$

where $K := \begin{bmatrix} k_1 & k_2 & k_3 \end{bmatrix}$ is the gain vector. The problem, however, is that the equilibrium point would be $(A - BK)^{-1} Bk_1 e = \begin{bmatrix} 0 & 0 & -\frac{k_1}{k_3} \end{bmatrix}^\top e$.

Therefore, the stabilization goal $|x| \to 0$ is not achieved under the control law (10). In order to overcome the nonzero steady-state bodies C^1 and C^2 angle problem, we add an integral action. To this end, we introduce an auxiliary variable x_e defined as $\dot{x}_e := 0 - x_5$, where zero stays as the reference for x_5. Then the extended state-space model is

$$\begin{bmatrix} \dot{x} \\ \dot{x}_e \end{bmatrix} = \underbrace{\left[\begin{array}{ccc|c} & A & & 0_{3\times 1} \\ \hline 0 & 0 & -1 & 0 \end{array}\right]}_{A_e} \begin{bmatrix} x \\ x_e \end{bmatrix} + \underbrace{\begin{bmatrix} B \\ 0 \end{bmatrix}}_{B_e} u.$$

The pair A_e, B_e is controllable and we can design the extended control law

$$u_1 := -K_e \begin{bmatrix} y_1 & x_2 & y_2 & x_e \end{bmatrix}^\top = -K_e \begin{bmatrix} x^\top & x_e \end{bmatrix}^\top - k_{e,1} e, \tag{11}$$

where $K_e \in \mathbb{R}^{1\times 4}$. Then the closed-loop dynamics is

$$\begin{bmatrix} \dot{x} \\ \dot{x}_e \end{bmatrix} = (A_e - B_e K_e) \begin{bmatrix} x \\ x_e \end{bmatrix} - B_e k_{e,1} e,$$

and the equilibrium is

$$(A_e - B_e K_e)^{-1} B_e k_{e,1} e = \begin{bmatrix} 0 & 0 & 0 & -\frac{k_{e,1}}{k_{e,4}} \end{bmatrix}^\top e.$$

Thus, the state x converges to zero, while the integral action x_e ensures the equilibrium offset compensation.

3.1. Experimental validation

The hardware for the tests[1] (shown in Fig. 2) is assembled from off-the-shelf components. The hardware parameters are summarized in the Table 1. A STM32F746 discovery board was chosen as the main computing unit. We have chosen a small brushless motor to drive the wheel D, the frames C^1 and C^2 are actuated by Dynamixel MX106-R servo motors. The inclination angle as well as the angular velocity of the body B are measured with an IMU.

We have implemented the control law (11), Fig. 3 provides the angle measurements y_1 and the corresponding control signal u_1. The corresponding gain vector K_e was chosen to be equal to $[35, 4, -1, 0.3]$. Note that after two seconds of the experiment an external force was applied for a short period of time, and the system has successfully recovered after that.

4. Conclusion

The main contribution of the paper is the model (6) simple enough for analysis on paper. We have validated the model through a hardware implementation that achieves the stabilization goal $q_b = -\frac{\pi}{4} - e, \omega_a = 0, \omega_b = 0$. Note that, while the pendulum is stabilized in the unstable equilibrium position, the proposed control law does not allow to control the angle q_a. Straightforward linearization techniques fail when $q_a = 0$ is added to the control goal; as a further research direction, we intend to study the possibility of full control of the system state.

[1] We have filmed the experiment, the video is available here: `https://youtu.be/4eYPoMV1Sac`.

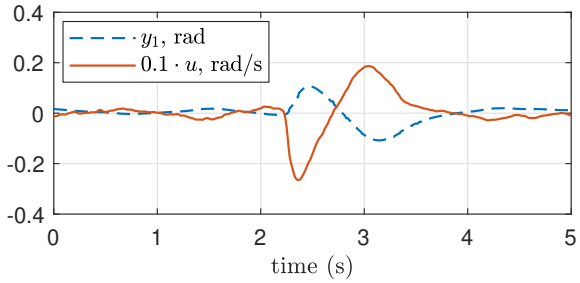

Fig. 3. Angle measurement y_1 and corresponding control u.

References

1. Inc., S.. Anti-roll gyro. `https://www.seakeeper.com/technology/`; cited November 2019.
2. Lee, S.D., Jung, S.. Awakening strategies from a sleeping mode to a balancing mode for a sphere robot. *International Journal of Control, Automation and Systems* 2017;**15**(6):2840–2847.
3. Chiu, J., Goswami, A.. Design of a wearable scissored-pair control moment gyroscope (sp-cmg) for human balance assist. In: *ASME 2014 international design engineering technical conferences and computers and information in engineering conference*. American Society of Mechanical Engineers; 2014, p. V05AT08A023–V05AT08A023.
4. Oya, H., Fujimoto, Y.. Preliminary experiments for postural control using wearable-cmg. In: *IECON 2017-43rd Annual Conference of the IEEE Industrial Electronics Society*. IEEE; 2017, p. 7602–7607.
5. Paradiso, J.A.. Global steering of single gimballed control moment gyroscopes using a directed search. *Journal of Guidance, Control, and Dynamics* 1992;**15**(5):1236–1244.
6. Thornton, B., Ura, T., Nose, Y., Turnock, S.. Zero-g class underwater robots: Unrestricted attitude control using control moment gyros. *IEEE Journal of Oceanic Engineering* 2007;**32**(3):565–583.
7. Sokolov, D., Aranovskiy, S., Gusev, A.A., Ryadchikov, I.. Experimental comparison of velocity estimators for a control moment gyroscope inverted pendulum, `https://hal.inria.fr/hal-02313600`; 2019. Working paper or preprint.
8. Aranovskiy, S., Ryadchikov, I., Nikulchev, E., Wang, J., Sokolov, D.. Experimental comparison of velocity observers: A scissored pair control moment gyroscope case study. *IEEE Access* 2020;**8**:21694–21702.
9. ECP (Educational Control Products), . Model 750: Control moment gyroscope. `http://www.ecpsystems.com/controls_ctrlgyro.htm`; cited November 2019.